Journal of Chemical Health Risks

www.jchr.org

JCHR (2025) 15(6), 2618-2633 | ISSN:2251-6727

Design, Development, and Optimization of Fluconazole Orodispersible Films Employing a Quality-by-Design Strategy

Mulchand Shende[1*], Dipali Madavi[2], Deepak Pawar[2]

[1]Government College of Pharmacy, Kathora Naka, Amravati, Maharashtra-444604, India.

[2]Department of Pharmaceutical Quality Assurance, Government College of Pharmacy, Kathora Naka, Amravati, Maharashtra-444604, India.

(Received: 25 October 2025 Revised: 27 November 2025 Accepted: 16 December 2025)

KEYWORDS

Orodispersible film, Fluconazole, Antifungal activity, release kinetics, Central Composite Design (CCD)

ABSTRACT:

Oral topical approaches have the advantage of targeted therapy and minimal side effects and are patient-friendly. This study aimed to develop thin, flexible, and transparent orodispersible films (ODFs) loaded with fluconazole (FCZ) for application to skin affected by fungal infections. A Quality by Design (QbD) framework was employed to optimize film composition using a Design of Experiments (DoE) approach. Hydroxypropyl methylcellulose E50 (HPMC E50), sodium alginate (SA), and polyethylene glycol 400 (PEG 400) were selected as formulation excipients, and their concentrations were systematically varied to evaluate their effects on critical quality attributes including folding endurance, drug release, and disintegration time. Nine formulations were prepared and assessed for physicochemical properties such as uniformity, mechanical strength, swelling index, and antifungal activity. FTIR and DSC analyses revealed no significant interactions between FCZ and the polymers, while drug loading efficiency confirmed uniform drug distribution within the films. The optimized formulation contained 2% w/v HPMC E50, 2% w/v SA, and 1.5% w/v PEG 400, achieving a folding endurance of 81.3, a disintegration time of 21 seconds, and a T‰% of 18.81 minutes. These results suggest that the developed FCZ-loaded orodispersible films are promising for effective, targeted antifungal therapy with enhanced patient compliance and minimal systemic side effects.

Introduction:

Over the past few decades, drug delivery technologies have evolved significantly. Oral drug delivery remains the conventional and most favoured method of drug administration. Most patients and healthcare providers prefer oral drug administration due to its convenience, cost-effectiveness, and enhanced treatment adherence. Among the various oral dosage forms, orodispersible films (ODFs) have recently attracted considerable interest because they dissolve or disperse quickly in the mouth, allowing for rapid action without the need for water. This characteristic is especially advantageous for patients who struggle to swallow traditional tablets or capsules, including children, the elderly, and those with dysphagia [1]. Oral candidiasis (OC), primarily caused by an overgrowth of *Candida* species, particularly *Candida albicans*, is a significant oro-pharyngeal antifungal condition [2].

Fluconazole (FCZ), an antifungal agent belonging to the bis-triazole derivative class, is primarily used to treat oral candidiasis. The molecular mass of FCZ is 306.27 g/mol, and it functions as a weak base with a pKa of 1.76 [3]. Reports indicate that the solubility of FCZ in water is 5 mg/ml[4]. Various polymorphic forms of FCZ have been identified, such as monohydrate, anhydrous form I, and anhydrous form II [4], along with several reported solvates of FCZ [5-7]. The anhydrous form II of FCZ exhibited higher water solubility and a faster intrinsic dissolution rate compared to anhydrous form I, while the lowest values for both characteristics were observed in the FCZ monohydrate [4].

Pharmaceutically, FCZ is commonly marketed as oral capsules for OC treatment. The minimum inhibitory concentration (MIC) of FCZ against *C. albicans* ranges from 2 to 16 µg/ml, and studies indicate that MIC values decrease as the medium's pH increases (typically between pH 4 and 7). Thin films infused with FCZ have

Journal of Chemical Health Risks
www.jchr.org
JCHR (2025) 15(6), 2618-2633 | ISSN:2251-6727

been created using both synthetic and natural polymers that possess mucoadhesive properties and have been studied for their application in oral candidiasis [8-10]. Regrettably, there is a lack of published research on protein films containing FCZ for treating oral candidiasis. Traditionally, FCZ has been administered in the form of oral tablets or capsules, which may not be suitable for patients who have difficulty swallowing or require rapid relief [11]. Oral administration requires a high dose of drug to reach the minimum fungal concentration, but this increases the risk of liver and kidney toxicity [12-13]. In this context, oral topical administration of FCZ represents the most favourable treatment modality for fungal infections. In order to increase the bioavailability of drugs, increasing solubility must be considered, and a feasible method is that of micellar solubilization with surfactants [14].

ODFs, derived from transdermal patch technology, consist of thin polymeric films that rapidly hydrate when placed on the tongue or other oral mucosal surfaces. Upon contact with saliva, the film disintegrates and releases the drug for mucosal or gastrointestinal absorption [15]. The buccal mucosa offers distinct advantages as a drug-delivery route: its permeability is estimated to be nearly 4000-fold higher than that of the skin, enabling efficient drug absorption while bypassing the gastrointestinal tract and avoiding first-pass hepatic metabolism [16-17].

In the present study, Quality by Design (QbD) principles were employed to optimize the formulation of the orodispersible film using Design-Expert Software version 12, incorporating two film-forming agents, HPMC E50 and Sodium Alginate, along with a plasticizer. A quality target product profile (QTPP) was established, and critical quality attributes (CQAs), including folding endurance, disintegration time, and T‰%, were identified. Response surface methodology was applied to assess the influence of critical process parameters (CPPs), particularly the concentrations of polymers and plasticizer, on these CQAs. The study aimed to refine the solvent-casting method for FCZ-loaded ODFs and comprehensively assess their physicochemical characteristics and antifungal performance for the treatment of oral candidiasis using a QbD-guided approach.

Materials and Methods:

All chemicals and reagents were procured from regional suppliers. Fluconazole (FCZ) was generously provided by Lupin Pvt. Ltd., Nagpur.

Selection of polymer and plasticizer

HPMC E50 and sodium alginate were selected as film-forming agents due to their excellent film-forming characteristics. Preliminary experiments revealed that polymer concentrations below 1.5% produced brittle films, while concentrations above 2.5% resulted in overly sticky films. Therefore, the polymer concentration range for ODF development was set between 1.5% and 2.5% w/v. Several plasticizers were evaluated, and polyethylene glycol 400 (PEG 400) produced the most favourable film characteristics. PEG 400 concentrations below 1% yielded films with low folding endurance; therefore, PEG 400 was used at concentrations ranging between 1–2% w/v.

Solubility determination and solubility enhancement

To determine solubility, an excess quantity of FCZ was added to 10 ml of each solvent in separate glass-stoppered tubes. The tubes were placed in a water-bath shaker at 37°C for 24 hours. After equilibrium was reached, solutions were filtered through Whatman filter paper, suitably diluted with distilled water, and analysed using a UV spectrophotometer [18]. Solid dispersions were prepared by dissolving FCZ and hydrophilic adsorbent carriers (HPMC E50 and sodium alginate) in minimal ethanol as per the weight ratios listed in Table 1. The solvent was evaporated under reduced pressure at 37°C. The resulting solid mass was ground, sieved through mesh no. 80, and stored in a vacuum desiccator until use [19].

Table 1: Compositions of FCZ-Polymer mixtures for solubility enhancement

Batch	FCZ	HPMC E50	Sodium alginate
B-1	1	1	1
B-2	1	2	1
B-3	1	1	2
B-4	1	2	2

Drug-excipients compatibility study

Drug–excipient interactions were analysed using FTIR spectroscopy and differential scanning calorimetry

Journal of Chemical Health Risks
www.jchr.org
JCHR (2025) 15(6), 2618-2633 | ISSN:2251-6727

(DSC). Pure FCZ and its physical mixtures were scanned from 4000 to 600 cm^{-1} and spectral changes were evaluated [20-21].

DSC thermograms were recorded using a Hitachi 7020 DSC with Nexta software. Samples (1–4 mg) were heated at 5°C/min under nitrogen atmosphere. Indium (99.99%) was used for calibration [22].

Experimental Quality by Design

A 3^2 Central Composite Design (CCD) with 9 experimental runs was applied to evaluate two independent variables: polymer concentration (X_1) and plasticizer concentration (X_2). Dependent variables (responses) included folding endurance (Y_1), T_{90}% (Y_2), and disintegration time (Y_3). Factor levels for polymers (HPMC E50 + sodium alginate) were 1.5%, 2.0%, and 2.5% w/v; plasticizer levels were 1.0%, 1.5%, and 2.0% w/v. Table 2 presents the design layout. A second-order polynomial model was used to determine the effects:

$$Y = b_0 + b_1X_1 + b_2X_2 + b_3X_1X_2 + b_4X_1^2 + b_5X_2^2$$

ANOVA ($p<0.05$) assessed model significance. Response surface plots and contour diagrams were generated for visualization [1].

Preparation of FCZ orodispersible films (ODFs)

HPMC E50 and sodium alginate were dispersed in distilled water and stirred until a clear solution formed. PEG 400 was added, and the mixture allowed to stand for 3–4 hours for air-bubble removal. FCZ was dissolved in ethanol, then combined with the polymer mixture. The final volume was adjusted to 20 ml, stirred thoroughly, and cast into petri dishes. Films were dried at room temperature and inspected for uniformity and ease of removal [23]. Formulations were prepared according to CCD by varying polymer (1.5–2.5%) and plasticizer (1–2%) concentrations.

Evaluation of ODFs

Visual inspection

Films were examined for colour, transparency, and surface uniformity.

Determination of thickness and weight variation

The thickness of the ODFs was measured using a digital micrometer. Thickness measurements were conducted at five locations across the film, including the center and multiple corner points. The average thickness of the films was subsequently calculated [17]. For weight variation, three strips of individual batches of size 2×2 cm^2 were cut and weighed individually using digital balance and the average weights were calculated for weight variation test [24].

Folding endurance measurement and surface pH

It is determined by repeatedly folding a small strip of the film (2×2 cm^2) at the same place till it broke. Folding endurance is measured by the number of folds a film can withstand at the same location before it breaks [25].

Surface pH of the films was measured using a digital pH meter. Each film was placed in a Petri dish and moistened with phosphate buffer (pH 6.8) for one hour. A glass electrode was gently placed close to the film's surface, and the pH reading was recorded after allowing it to stabilize for one minute [25].

Determination of tensile strength and % elongation

Tensile strength of the Orodispersible films (ODFs) was assessed by subjecting them to mechanical stress. Film samples measuring 2×2cm^2 were positioned vertically between two clamps. The force at which the film began to tear was recorded. Tensile strength was defined as the maximum force necessary to rupture the film and was determined by dividing this force by the film's cross-sectional area [26].

Tensile strength = force at break (kg)/initial cross-sectional area of the sample (cm^2)

Percent elongation refers to the extent to which a film sample stretches under applied stress, known as strain. Strain is calculated as the change in length divided by the film's original length. Typically, the elongation increases with higher concentrations of plasticizer in the formulation [26].

% Elongation = Increase in length×100/Original length

Swelling index and water absorption ratio

Initially, a film sample measuring 2×2 cm^2 is weighed before being placed on a pre-weighed cover slip. This assembly is subsequently immersed in 20 ml of phosphate buffer (pH 6.8) within a beaker. At designated time intervals, the cover slip is carefully removed, and any excess moisture on its surface is gently absorbed with absorbent tissue. The weight gain of the film is

Journal of Chemical Health Risks
www.jchr.org
JCHR (2025) 15(6), 2618-2633 | ISSN:2251-6727

meticulously recorded at each interval until it reaches a stable state. The swelling index is then calculated using the appropriate formula [15].

Table 2: Ranges of dependent variables as per QbD

Std	X1	X2	FCZ (mg)	HPMC E50 and Sodium Alginate (% w/v)	Propylene Glycol 400 (% w/v)	Ethanol (ml)	Distilled Water q. s.
F1	1.5	1	159	1.5	1	3	20
F2	2.5	1	159	2.5	1	3	20
F3	1.5	2	159	1.5	2	3	20
F4	2.5	2	159	2.5	2	3	20
F5	1.2	1.5	159	1.2	1.5	3	20
F6	2.7	1.5	159	2.7	1.5	3	20
F7	2	0.7	159	2	0.7	3	20
F8	2	2.2	159	2	2.2	3	20
F9	2	1.5	159	2	1.5	3	20

$$SI = (Wt - Wo)/Wo$$

Where, SI = swelling index, Wt = weight of the film at time=t, and Wo = weight of the film at time t=0.

A piece of tissue paper, folded twice, is placed in a small petri dish with 10 ml of water. A 2x2 cm film is positioned on the paper, and the time taken for complete wetting is recorded. Subsequently, the wetted film is weighed. The water absorption ratio (R) is calculated using the following [27].

$$R = (Wa - Wb)/Wb \times 100$$

Where, Wb= weight of film before water absorption, Wa= weight of film after water absorption.

Drug content

An oral film measuring 2×2 cm² is dissolved in 100 ml of phosphate buffer with a pH of 6.8. The resulting solution is sonicated for 15 minutes and then filtered. The filtrate is suitably diluted and analyzed using a UV-visible spectrophotometer at its maximum absorbance wavelength (λ_{max}). Drug concentration is determined by referencing a previously prepared standard calibration curve [28].

Estimation of drug loading and entrapment efficiency

From each polymer film loaded with FCZ, three samples were taken from different places, over which phosphate-buffer solution (pH 6.8) was added. In order to release FCZ from the polymer network, the samples were placed in the ultrasonic bath for 60 min, then centrifuged for 15 min at 3500 rpm and filtered through Whatman filter paper. The supernatant was diluted to one of the concentrations on the calibration curve and analyzed quantitatively, using the developed spectrophotometric method. Following the spectral analysis, the amount of drug loaded in the polymer films was established. The formulas used for calculation of entrapment efficiency (EE) and loading capacity (LC) are as follows [29].

$$EE, \% = (mFCZexp/mFCZ^{th}) \times 100$$

EE - entrapment efficiency, %; mFCZexp - amount of FCZ loaded into the polymeric film; mg; $mFCZ^{th}$ - amount of FCZ that was added into the polymeric film; mg.

$$LC, \% = (mFCZexp/m_{polymeric\ film}) \times 100$$

LC-loading capacity of FCZ in polymeric films; FCZ - amount of FCZ loaded into the polymeric film; mg; $m_{polymeric\ film}$ - mass of the polymeric film; mg.

Disintegration time and *In-vitro* release of FCZ ODFs

The disintegration time is assessed visually by immersing a film (2x2 cm²) in a petri dish containing 10 ml of phosphate buffer at pH 6.8, maintained at 37ºC. The petri dish is agitated every 10 seconds, and the time is recorded at the moment the film begins to break or

Journal of Chemical Health Risks
www.jchr.org
JCHR (2025) 15(6), 2618-2633 | ISSN:2251-6727

disintegrate. The disintegration time is defined as the duration until the film tears [22].

In-vitro drug dissolution testing is performed utilizing the USP Apparatus I (basket method) at a temperature of 37°C±0.5°C, employing 250 ml of phosphate buffer (pH 6.8) as the dissolution medium. A drug-loaded film measuring 2×2 cm² is immersed in the medium, while the basket is rotated at 50 rpm. At specified intervals, 5 ml samples are extracted and substituted with fresh dissolution medium. Subsequently, the samples are filtered using Whatman filter paper and analyzed spectrophotometrically at λ_{max} [15].

***Ex-vivo* permeation studies**

The prepared ODF strips are placed in a franz diffusion cell, resting on the upper membrane of the donor compartment. The receptor compartment holds 20 ml of phosphate buffer (pH 6.8), which is in contact with a dialysis membrane that has been pre-washed and soaked in the buffer. The donor compartment features a film measuring 2×2 cm. Additionally, the receptor compartment contains a magnetic bead, and the entire assembly is set on a magnetic stirrer. Once the film is in place, the drug begins to diffuse through the dialysis membrane into the receptor compartment. At 5-minute intervals, 2 ml samples are collected for up to 60 minutes, ensuring sink conditions by replacing the withdrawn volume with an equal amount of fresh phosphate buffer (pH 6.8). The samples are then analyzed at regular intervals by measuring absorbance at λmax using a UV spectrophotometer to determine the percentage of drug that has permeated [24].

Antifungal activity

The antifungal effectiveness of FCZ was evaluated using the Combined Microbial Sensitivity Discs method (CLAIRO® COMBI), which provides a semi-quantitative assessment of *in-vitro* susceptibility to antimicrobial agents. To prepare the agar plates, pour sterile Mueller-Hinton agar with a pH of 7.3 ± 0.1 into petri dishes, ensuring a depth of approximately 4 mm, and incubate at 35°C for 30 minutes to eliminate moisture. For inoculum preparation, use a pure bacterial culture, verifying its purity through Gram staining. Transfer 4-5 similar colonies into 5 ml of tryptic soy broth and incubate at 35–37°C for 2-5 hours until moderate turbidity is achieved. Adjust the culture to a 0.5 McFarland standard by diluting it with sterile broth or saline. Inoculate the agar by spreading the diluted culture with a sterile cotton swab in three directions, rotating the plate 60° between each streak. Allow the plates to dry for 5-10 minutes, then place a combi disc on the surface and let it rest for 30 minutes at room temperature. Incubate the plates at 35–37°C for 16-18 hours. Assess the zones of inhibition and document their diameters in millimetres. In urgent situations, the plates may be read after 6-8 hours, but only zones of complete inhibition should be measured. If isolated colonies appear instead of uniform growth, the inoculum was too light, and the test should be repeated [30-31].

Stability studies

The stability study of the prepared films was carried out by storing films in an aluminium package for 60 days at 40±0.5°C with 75±5% RH. The films were observed for physical changes, weight, thickness, drug content, folding endurance, *in-vitro* disintegration time, surface pH, swelling index, water absorption ratio, tensile strength, and percentage elongation [28].

Data analysis

The evaluation's data were statistically examined using ANOVA. Design expert software used for the analysis of data. It was applied to assess the importance and size of the impacts of various variables and how they interacted. It was decided that a probability value was statistically significant when it was less than 0.05.

Results and Discussion:

The saturation solubility of FCZ and polymer-based solid dispersions in water and phosphate buffer (pH 6.8) is listed in Table 3.

Table 3: Solubility of Fluconazole in Different Polymer Ratios

Batch	FCZ: HPMC E50:SA	Water (µg /ml)	Phosphate Buffer pH 6.8 (µg /ml)
Pure Drug	-	26.96 ± 0.5	56.09 ± 0.6
B-1	1:1:1	45.87 + 1.4	56.89 + 1.3
B-2	1:2:1	57.92 ± 1.4	68.96 ± 1.7
B-3	1:1:2	60.23 ± 1.2	71.97 ± 1.6
B-4	1:2:2	71.98 + 1.2	80.98 + 2.3

Journal of Chemical Health Risks
www.jchr.org
JCHR (2025) 15(6), 2618-2633 | ISSN:2251-6727

Pure FCZ exhibited solubility of 26.96 ± 0.5 µg/mL (water) and 56.09 ± 0.6 µg/mL (PBS). Among all batches, B-4 (1:2:2) showed the highest solubility, achieving 71.98 ± 1.2 µg/mL in water and 80.98 ± 2.3 µg/mL in PBS.

Drug-excipients interaction study

The FTIR spectra of FCZ, the individual polymers, the physical mixture, and formulation are presented in Figure 1, with peak assignments summarized in Table 4. All characteristic peaks of FCZ including aromatic C–H stretching (3108–3021 cm^{-1}), aromatic C=C stretching (1596–1616 cm^{-1}), C–N stretching (1372 cm^{-1}), and ether C–O–C stretching (1138–1010 cm^{-1}) were retained in the physical mixture and final formulation. No significant peak shifts or disappearance was detected, indicating the absence of chemical interactions and confirming compatibility between FCZ and the selected excipients.

Table 4: FTIR data for FCZ, polymers, and physical mixture

Functional groups (cm^{-1})	Standard Wave numbers	FCZ	Physical Mixture	Formulation
Aromatic C–H Stretch	3000-3100	3108–3021	3108–3021	3108–3021
Aromatic C=C Stretch	1596-1616	1616	1596	1596
N–H Bend / Amine Stretch	1550-1650	1503	1450–1437	1450–1437
C–N Stretch	1200-1350	1372	1372	1372
C–O–C Stretch (Ether)	1000-1300	1138–1018	1134–1010	1138–1010
Aromatic C–H Bending	650-900	964–831	914	914

DSC thermograms (Figure 2) revealed a sharp endothermic peak for FCZ at 139 °C (133 mJ/mg), confirming its crystalline nature. HPMC E50 showed transitions at 215.7–218.9 °C and 224 °C, while sodium alginate exhibited moisture loss at 48.4 °C, relaxation at 117.1 °C, and degradation at approximately 200.2 °C. The physical mixture maintained characteristic FCZ peaks at 134.8 °C and 139.1 °C, confirming the absence of significant drug–polymer interaction. These results validate the chemical stability of FCZ in the polymeric environment.

DSC thermogram of B-4 (Figure 3) showed complete disappearance of FCZ's melting peak, suggesting conversion to an amorphous or molecularly dispersed form. This transformation enhances wettability and dissolution, which accounts for the improved solubility. Similar observations were reported by Shinde et al. for solid-dispersion-based solubility enhancement [18]. To investigate the mechanism behind the enhanced solubility observed in batch 4, DSC analysis was carried out. The Thermogram of pure Fluconazole exhibited a sharp endothermic peak at approximately 138–140°C, corresponding to its melting point, which confirmed its crystalline nature as shown in Figure 3. In contrast, the DSC Thermogram of batch 4 did not show this characteristic melting peak. The absence of this endothermic transition indicated that Fluconazole was no longer present in its crystalline form in the formulation. Instead, the drug may have been converted into an amorphous form or molecularly dispersed within the hydrophilic polymeric matrix.

This transformation was likely responsible for the enhanced solubility, as the amorphous form typically possesses higher free energy, improved wettability, and greater dissolution rates compared to the crystalline form. The DSC results thus supported the formation of a solid dispersion system in batch 4, aligning with the observed increase in solubility. These solubility enhancement study align with the work of Shinde et al., who developed different binary polymer mixture for solubility enhancement of poorly water-soluble drug by solid dispersion technique [18].

Formulation development and experimental design

Orodispersible films (ODFs) were prepared using varying concentrations of Hydroxypropyl methylcellulose (HPMC E50) and sodium alginate (SA) within the range of 1.5–2.5% w/v, along with polyethylene glycol 400 (PEG 400) between 1–2% w/v. The films were successfully produced via a physical cross-linking mechanism driven by inter- and intramolecular hydrogen bonding, resulting in smooth, uniform films with desirable flexibility. A Central Composite Design (CCD) was used to study the effects of polymer concentration (X_1) and plasticizer -

Journal of Chemical Health Risks
www.jchr.org
JCHR (2025) 15(6), 2618-2633 | ISSN:2251-6727

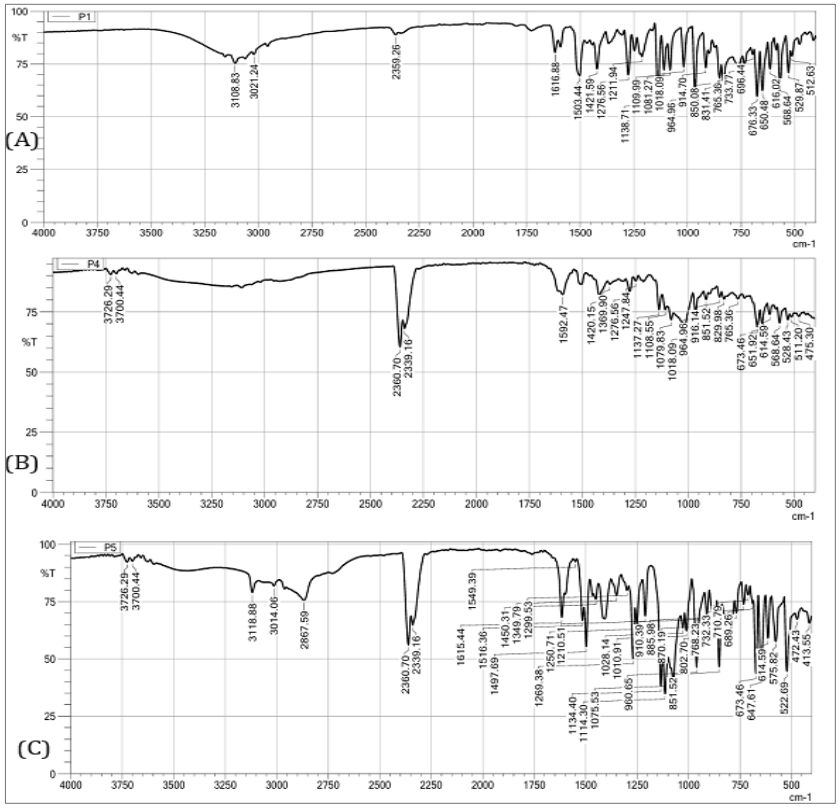

Figure 1: IR spectra of FCZ API, physical mixture of FCZ and excipients, and formulation F9, (A) IR spectrum of FCZ. (B) IR spectrum of physical mixture and (C) IR spectrum of formulation (F9)

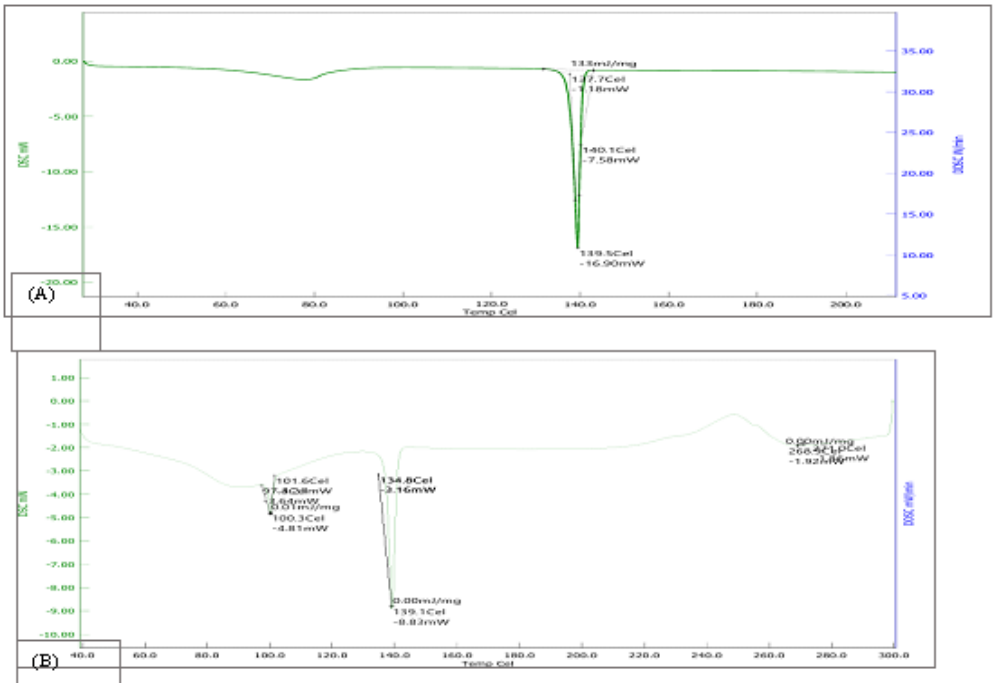

Figure 2: DSC of FCZ API, physical mixture of FCZ and excipients, and formulation F9, (A) DSC of FCZ and (B) DSC of physical mixture

Journal of Chemical Health Risks
www.jchr.org
JCHR (2025) 15(6), 2618-2633 | ISSN:2251-6727

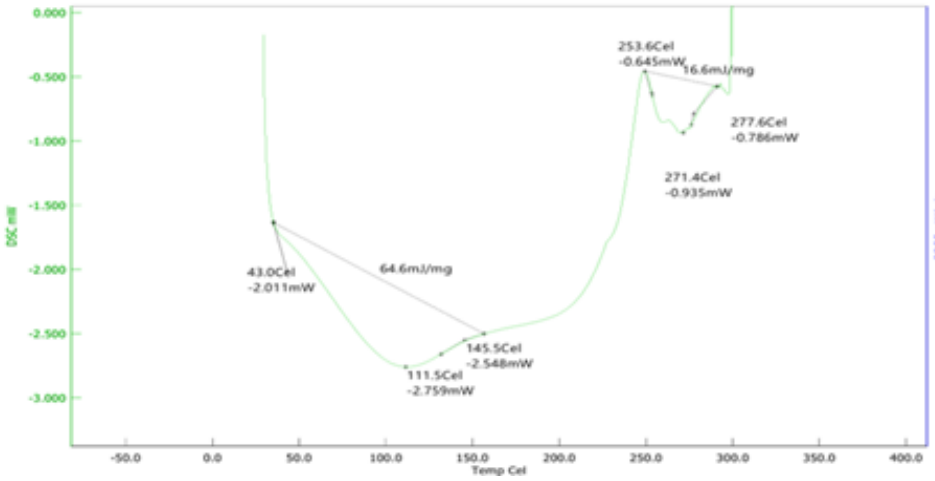

Figure 3: DSC of ODFs

-concentration (X_2) on folding endurance (Y_1), disintegration time (Y_2), and T_{90}% (Y_3). Experimental outputs are presented in Table 5.

Optimization data analysis

Using the Design Expert® Version 12 software, batches were formulated suggested by DoE and assessed. Various independent variables have significant effect on the dependent variables. Independent variables were polymer and plasticizer concentration and dependent variables were folding endurance, disintegration time (sec) and T_{90}% (time required to release 90% of drug release in minutes). Total 9 runs carried out which were provided by DoE software. ANOVA employed to check the consequence and the effects of independent variables on the folding endurance, disintegration time and T_{90}%. ANOVA for response 1- folding endurance shown in (Table 5). The polynomial equation obtained for folding endurance Y_1 is as follows:

$$Y_1 = 79.60+3.07X_1-0.1726X_2+0.1750X_1X_2-1.99X_1^2-0.1625X_2^2$$

The folding endurance of film was increases as the amount of polymer increases. In above polynomial equation for Y_1 response, b1 with positive value was obtained which described increase in concentration of factor X_1 (HPMC E50 LV), there was increase in response Y_1 (Y_1= Folding Endurance). Coefficient b2 with negative value for Y_1 was obtained which describe increase in concentration of factor X_2 (propylene glycol 400), there was decrease in response Y_1. The Model F-value of 6.97 implies the model is significant $p< 0.0127$. The contour and 3D Surface plots (Figure 4) showed the effect of different independent variables on folding endurance (Y_1). The polynomial equation for the Y_2 response, which measures *in-vitro* disintegration time, yielded a positive coefficient b1 of +0.73 and b2 of +1.58. This indicates that as the concentration of factor X_1 (HPMC E50 and SA) and X_2 increases, the Y_2 response also increases. Consequently, this implies that larger quantities of the polymer produce films that require more time to disintegrate.

$$Y_2 = 21+0.73X_1+1.58X_2-0.25X_1X_2+3.06X_1^2+1.56X_2^2$$

The negative interaction term b3 (–0.25) indicates a slight antagonistic interaction between the two polymers suggesting that when both are increased together, the combined effect on disintegration time is slightly reduced. Furthermore, the positive quadratic coefficients b4 (+3.06 for X_1^2) and b5 (+1.56 for X_2^2) indicate that at elevated concentrations of both the polymer and plasticizer, the response surface exhibits an upward curvature. This implies that disintegration time may increase more significantly at extreme concentrations, especially for the plasticizer, where the initial downward trend is reversed due to the pronounced quadratic effect (Figure 4). These findings imply that moderate polymer levels favour optimized disintegration, while excessive polymer content may increase viscosity and hinder disintegration. The model was statistically significant (F-value = 392.66, $p<0.0001$). Contour and 3D surface plots confirmed the interactive influence of both factors on in-vitro disintegration time.

$$Y_3 = 18.81-0.4982X_1-0.3305X_2+0.2875X_1X_2+0.8150X_1^2+0.3175X_2^2$$

Journal of Chemical Health Risks
www.jchr.org
JCHR (2025) 15(6), 2618-2633 | ISSN:2251-6727

In the above polynomial equation for the Y3 response (T_{90}%), The negative coefficient b1 (−0.4982) for polymer indicates that increasing its concentration decreases T90%, promoting faster drug release. Similarly, the negative coefficient b2 (−0.3305) for plasticizer shows that higher levels also reduce T_{90}%, accelerating release. Positive quadratic coefficients (b4 and b5) suggest that at higher concentrations of both factors, T_{90}% increases again, indicating slower release. The positive interaction term b3 (+0.2875) implies a combined effect of polymer and plasticizer, slightly increasing T_{90}% at elevated concentrations. Initially, both factors decrease T_{90}%, but nonlinear effects at higher levels lead to a slower release rate due to increased matrix density. The Model F-value of 5.45 implies the model is significant $p<0.0231$ shown in Table 6. To illustrate the relationship between the independent variables and the responses, 2D contour plots and 3D response surface plots were generated using Design Expert software version 12 and are presented in Figure 4. The overlay plot (Figure 5) highlights the design space meeting all response criteria. The optimized formulation 2% polymer and 1.5% PEG 400 fell entirely within the acceptable region and corresponded to batch F9. The overlay plot (Figure 5) illustrates the combined effects of polymer concentration (X_1) and plasticizer concentration (X_2) on folding endurance (Y_1), disintegration time (Y_2), and T_{90}% (Y_3). The yellow region represents the design space where all three responses fall within the desired limits, indicating successful formulation performance. The red dots correspond to the experimental design points. Among these, the optimized solution, located at 2% polymer and 1.5% plasticizer, lies within the acceptable yellow region and was identified as the optimized batch based on desirability criteria. This confirms that F9 meets the required balance of mechanical strength, rapid disintegration, and drug release. The overlay plot thus supports the selection of formulation F9 as the optimal combination within the experimental range these finding align with Sharma et al.,[32]. Based on the results of ANOVA and model analysis, the optimal experimental conditions were identified by analysing the interaction effects and response surface plots.

Table 5: Runs and responses for ODFs

Formulation	FCZ (mg)	Factor 1	Factor 2	Response 1	Response 2	Response 2
		Polymer (X_1)	Plasticizer (X_2)	Folding endurance (Y_1)	*In-vitro* Disintegration time (sec) (Y_2)	%T_{90} (min) (Y_3)
F1	159	1.5	1	71.6±3.05	23±4.72	20.73
F2	159	2.5	1	78.6±1.52	25±1.52	20.05
F3	159	1.5	2	73.6±4.16	27±3.60	19.71
F4	159	2.5	2	79.6±5.03	28±2.64	20.18
F5	159	1.2	1.5	73.3±4.16	26±3.50	21.55
F6	159	2.7	1.5	80.3±4.50	28±5.03	18.88
F7	159	2	0.7	82.6±4.50	22±4.2	19.84
F8	159	2	2.2	78.3±3.05	26±4.7	18.6
F9	159	2	1.5	81.3±1.52	21±4.11	18.81

Table 6: ANOVA analysis of response (Polymer concentration and plasticizer concentration)

Responses	Folding endurance (Y_1)		Disintegration time (Y_2)		%T_{90} (Y_3)		Remarks
Source	F-value	P-value	F-value	P-value	F-value	P-value	
Model	5.09	0.0274	392.66	< 0.0001	5.45	0.0231	significant
A-X1(Polymer con.)	18.61	0.0035	83.92	< 0.0001	6.66	0.0364	
B-X2(Plasticizer con.)	0.0587	0.8156	395.6	< 0.0001	2.93	0.1307	
AB	0.0301	0.8671	4.94	0.0616	1.11	0.3274	
A^2	6.76	0.0354	1289.47	< 0.0001	15.49	0.0056	
B^2	0.0452	0.8377	335.66	< 0.0001	2.35	0.169	

Journal of Chemical Health Risks
www.jchr.org
JCHR (2025) 15(6), 2618-2633 | ISSN:2251-6727

These conditions corresponded to the formulation variables that provided the most desirable outcomes for the targeted responses. This condition is optimized and X_1 (Polymer concentration) (2 %w/v) and X_2 (Plasticizer concentration) (1.5 %w/v) selected as it provides most desirable and reliable formulation responses. By using above optimized condition formulation was developed and evaluated for different parameter.

Model validation

To obtain maximum folding endurance and T_{90}% (min), and minimum *in-vitro* disintegration time software suggested a formulation and selected for the further evaluation. The observed values were compared with the predicted values. Predicted and observed values (Table 7) showed <5% relative error for all three responses, confirming excellent model accuracy and predictive capability.

The predicted and experimental values for folding endurance (1.33%), *in-vitro* disintegration time (0.33%), and T90% (3.83%) were compared to validate the accuracy of the developed formulation model. The relative errors for all three parameters were found to be below 5%, indicating a high degree of predictive accuracy. Moreover, all observed values fell within their respective 95% confidence intervals and 99% tolerance intervals, confirming that the model predictions are statistically reliable and robust. These findings support the model's suitability for guiding formulation optimization. The close alignment between predicted and actual outcomes demonstrates the model's capability to accurately forecast key performance metrics of the formulation. This result is consistent with previous research by Shakya et al., who reported successful model validation using Response Surface Methodology in the development of Sitagliptin Phosphate tablets [33].

Characterization of ODFs

FCZ orodispersible films prepared were transparent, colorless, thin, and soft, with no spot on the film surface. Physicochemical evaluation data are presented in Tables 8. The prepared orodispersible films (F1–F9) demonstrated good uniformity and desirable physicochemical properties. The film weights ranged from 11±1 mg (F1) to 26±1 mg (F2), and thickness varied between 0.21±0.040 mm (F5) and 0.28 ± 0.055 mm (F6), indicating consistent formulation. Drug content was uniformly distributed, ranging from 84.47±0.01% to 96.20 ± 0.04%, and surface pH remained within a neutral range (6.56±0.04 to 6.86±0.03), ensuring compatibility with the oral mucosa.

Folding endurance improved with increasing polymer concentration, ranging from 71.6±3.05 (F1) to 81.3±1.52 (F9). The swelling index ranged from 2.21±0.99 (F5) to 3.76±0.39 (F4), while the water absorption ratio varied from 190.3±2.8 (F3) to 374.4±6.4 (F5), both showing a trend of increase with higher polymer and plasticizer content. In vitro disintegration time was rapid for all formulations, with the shortest being 23±2.64 seconds (F4) and the longest 61±3.60 seconds (F3); faster disintegration correlated with higher polymer concentrations. Overall, the films exhibited promising characteristics suitable for fast oral delivery.

The entrapment efficiency (EE) and loading capacity (LC) of the drug in the polymeric films were determined by using UV Spectrophotometric method. The wavelength at which fluconazole absorbs in phosphate buffer (pH 6.8) is 261 nm, the range of linearity is 10–100 µg/ml, and the regression coefficient is 0.9944, a value close to unity, which indicates compliance with Beer's law in the chosen concentration range, and the value of significance is equal to 5.43×10^{-13} [34-35]. Calculation of the amount of drug loaded was performed by using absorbance=0.0019×concentration+0.0046. The loading efficiency results of over 95% indicate a uniform distribution of the drug in both formulations, which suggests a high compatibility between the ingredients of the polymer films. The films have a large amount of drug per 1 cm^2 surface area, so the treatment of fungal infections can be adapted depending on the affected skin area.

***In-vitro* drug release**

Figure 6 is illustrating the cumulative percentage of drug release data for formulations F1 through F9. Formulations F2, F6, F7, F8, and F9 demonstrated superior drug release rates of 92.82%, 91.74%, 92.49%, 96.20%, and 95.91% respectively at 20 minutes. Therefore, the results indicate that an increase in polymer concentration correlates with a rise in cumulative percentage drug release. The release kinetics of orodispersible film formulations (F1 to F9) were evaluated through various kinetic models, such as zero-order, first-order, Higuchi, Korsmeyer-Peppas, and

Journal of Chemical Health Risks
www.jchr.org
JCHR (2025) 15(6), 2618-2633 | ISSN:2251-6727

quadratic models. The analysis was conducted using DD Excel software, which generated release constants and R^2 values for each model. Zero-Order Model demonstrated moderate to high R^2 values ranging from 0.9275 to 0.9926, indicating some relevance to the release kinetics. First-Order Model exhibited low and inconsistent R^2 values between 0.7897 and 0.9134, suggesting a poor fit. Higuchi Model displayed a weak fit with R^2 values from 0.6554 to 0.8362, reflecting limited relevance to the formulation. Korsmeyer-Peppas Model offered the best fit with R^2 values spanning 0.9777 to 0.9964, indicating an excellent statistical fit, thus making it the most appropriate model for describing the release mechanism, which involves both diffusion and polymer erosion. Quadratic Model showed a strong fit with R^2 values between 0.9790 and 0.9932, particularly for formulations exhibiting initial burst release, although it did not capture the release mechanisms as effectively as the Korsmeyer-Peppas model. Cumulative release profiles (Figure 6) showed that F2, F6, F7, F8, and F9 exhibited >90% release within 20 minutes. F9 demonstrated 95.91% release at 20 minutes and the lowest T_{90}%. Kinetic modelling revealed Korsmeyer–Peppas model provided the best fit (R^2 = 0.9777–0.9964), indicating release via diffusion coupled with polymer erosion. Ranking based on best model fit: F9>F5>F8>F3>F2>F6>F1>F7>F4.

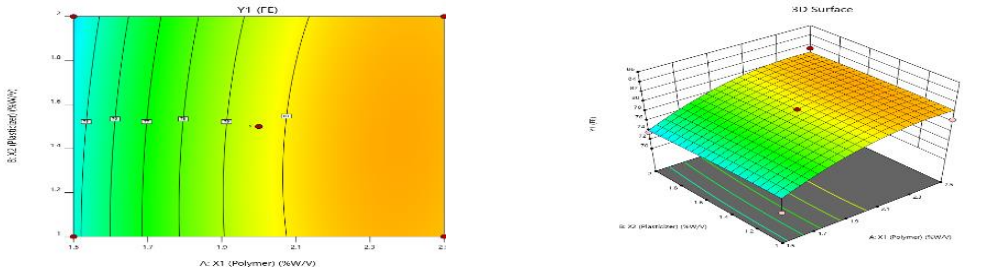

(a) Counter and 3D plot showing folding endurance (Y_1)

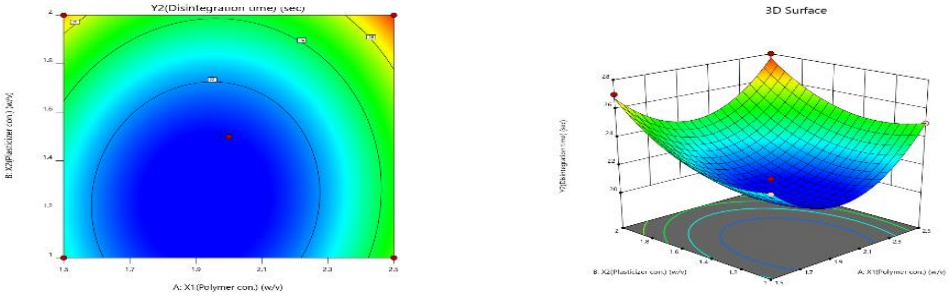

(b) Counter and 3D plot showing disintegration time (Y_2)

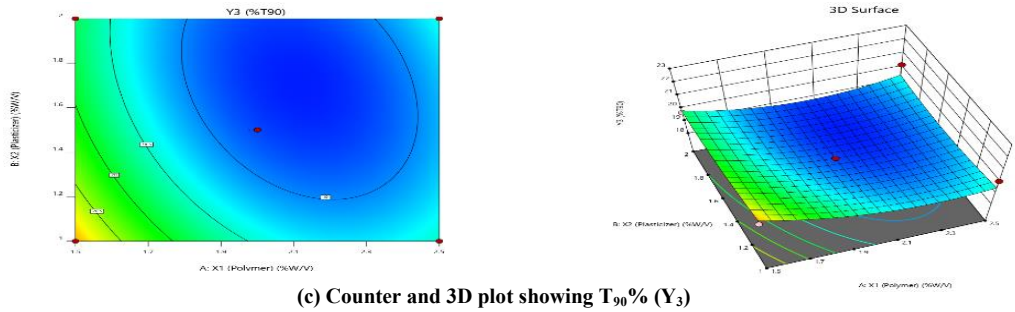

(c) Counter and 3D plot showing T_{90}% (Y_3)

Figure 4: Contour and 3D Surface plot showing the effect of polymer concentration (X_1) and plasticizer concentration (X_2) on response

Journal of Chemical Health Risks
www.jchr.org
JCHR (2025) 15(6), 2618-2633 | ISSN:2251-6727

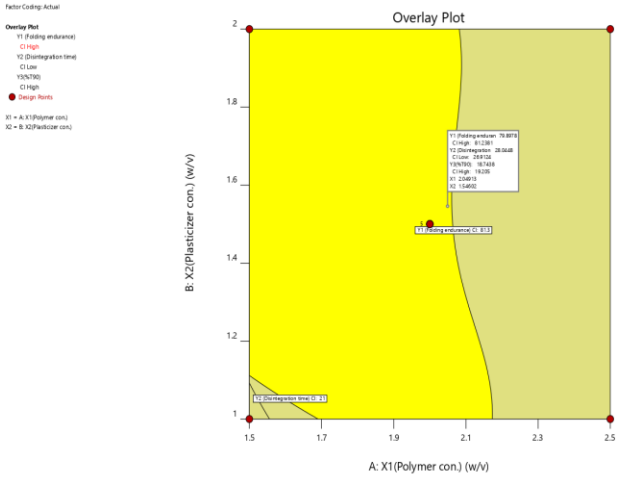

Figure 5: The overlay plot features a yellow-shaded region representing the design space, with the optimized formulation composition indicated by a flagged point

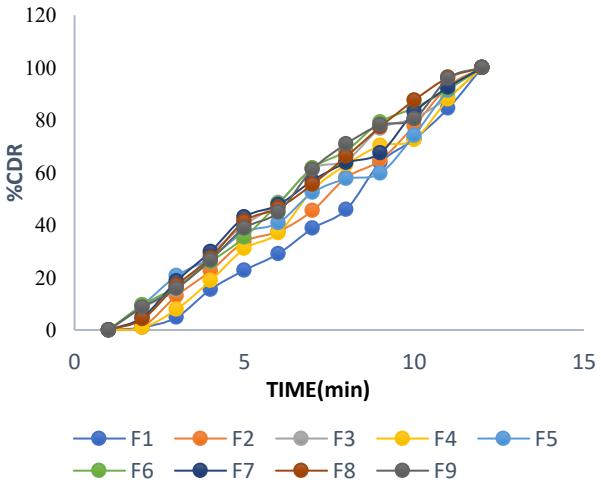

Figure 6: *In-vitro* drug release study of ODFs (F1-F9)

***In-vitro* permeation and antimicrobial activity**

Ex-vivo transmucosal permeation studies were conducted using an egg shell membrane to evaluate FCZ delivery from orodispersible films formulated with HPMC E50+SA, and PEG 400. The permeability of the orodispersible film formulations (F9) was evaluated by quantifying the cumulative drug permeation per unit area (CADD) over a duration of 65 minutes. F9 formulations demonstrated a swift and continuous increase in drug permeation through the membrane. The initial permeation recorded was 2.65% at the 5-minute mark (Table 9). Notably, formulation F9, which contained 2% w/v of HPMC E50 and SA, achieved the highest drug permeation rate of 90.19% within 60 minutes. The *ex-vivo* study results indicated that FCZ from orodispersible films can effectively transport the drug across the mucosal membrane of the pregastric route, which includes the mouth, pharynx, and oesophagus, thereby making them ideal for rapid trans mucosal delivery.

The optimized formulation F9 demonstrated the highest permeation performance, with a diffusion rate of 0.1117 µg/h and a permeability coefficient of 0.0117 cm/h (11.7×10^{-3}), likely due to enhanced solubilization and membrane interaction effects of PEG 400.

The optimized polymeric films were evaluated against the clinical strain *Candida albicans* SC5314. Table 9 provides details on the antifungal efficacy measured by the zones of inhibition (in mm), with results reported as means±SD. Polymeric films loaded FCZ demonstrate notable antimicrobial effectiveness against Candida albicans SC5314. The conducted tests revealed that the inhibition zone diameter of the FCZ-loaded polymeric films (F9) increases slightly with higher drug concentrations in the samples. These antifungal findings align with the work of Kraisit, P et al., who developed FCZ-loaded solid lipid nanoparticles incorporated into chitosan films using the film casting technique [36]. Collectively, these findings indicate that polymer films containing FCZ as an active ingredient hold potential for treating fungal infections.

Stability studies

The optimized batch F9 was evaluated for stability over 60 days under real-time (40± 2°C/75% ± 5% RH). Parameters assessed included appearance, weight, thickness, drug content, folding endurance, *in-vitro* disintegration time, surface pH, swelling index, water absorption ratio, tensile strength, and % elongation. No significant changes were observed in any parameter under either condition. After 60 days of storage (40±2 °C, 75±5% RH), no significant changes were observed in physicochemical parameters (Table 10). Drug content, mechanical strength, disintegration, and physical appearance remained stable, confirming the robustness of the optimized formulation.

Journal of Chemical Health Risks
www.jchr.org
JCHR (2025) 15(6), 2618-2633 | ISSN:2251-6727

Table 7: Predicted and observed responses for the optimized formulation (Mean ± S.D.), *n=3*

Solution	Predicted Mean	Predicted Median	Observed	Std Dev	SE Mean	95% CI low for Mean	95% CI high for Mean	95% TI low for 99% Pop	95% TI high for 99% Pop	Relative error (%)
Folding endurance	80.23	80.23	81.30	2.01617	0.887711	78.1379	82.3361	69.222	91.252	1.33%
In-vitro disintegration time (sec)	21.08	21.08	21.15	0.22494	0.0990398	20.8556	21.324	19.8609	22.3187	0.33%
T90% (min)	18.80	18.80	18.08	0.54612	0.240454	18.2397	19.3769	15.8247	21.792	3.83%

Table 8: Data of evaluation parameters of FCZ (Mean±Std) *n=3*

Batch	F1	F2	F3	F4	F5	F6	F7	F8	F9
Weight (mg)	11±1.2	26±1.1	15.33±1.5	20.66±1.4	14.66±1.1	20.33±2.05	19±2	21±2.2	18±1.6
Thickness (mm)	0.23±0.03	0.26±0.06	0.25±0.05	0.24±0.05	0.21±0.04	0.28±0.05	0.22±0.044	0.25±0.062	0.23±0.03
Drug Content (%)	84.47±0.01	92.8±0.07	88.66±0.03	88.01±0.02	91.11±0.13	91.74 ±0.05	92.49 ±0.05	96.20 ±0.04	95.91 ±0.01
Surface pH	6.67± 0.05	6.82± 0.04	6.69± 0.08	6.7± 0.02	6.56± 0.04	6.75± 0.03	6.81±0.01	6.86±0.03	6.79±0.06
Tensile strength (N/cm)	0.081	0.093	0.079	0.086	0.081	0.092	0.078	0.088	0.085
% Elongation	24.34	22.34	28.34	21.67	13.34	21.67	17.34	19	32
Swelling Index	2.98± 0.40	2.48± 0.18	2.25± 0.66	3.76± 0.39	2.21± 0.99	2.98± 0.40	2.46± 0.14	2.48± 0.36	2.47± 0.12
Water absorption ratio	244.4±1.1	226.3±2.9	190.3±2.8	258.9±3.9	374.4±6.4	356.7±1.3	252.2±6.0	255.9±4.1	254.4±2.3
LC (±SD) %	32.07±0.006	42.56±0.005	41.67±0.002	39.15±0.006	39.46±0.003	36.63±0.008	40.62±0.006	39.36±0.004	40.30±0.001
EE (±SD) %	99.35±0.04	98.30±0.03	93.62±0.04	98.00±0.02	97.94±0.01	90.53±0.05	90.89±0.03	98.03±0.07	99.46±0.01

Table 9: Permeability parameter of FCZ and antimicrobial sensitivity test against *Candida albicans* SC5314 fungi stains (After 24 hours at 37°C)

Form/Batch	Area of D.M ($Cm^{2)}$	Film Thickness (mm±SD)	Diffusion Rate (µg/cm2/min)	Permeability Coefficient (cm/min)	ZOI (mm)
FCZ (10 mg)	7.069	0.25 ± 0.02	0.2888±0.033	$5.77±0.025×10^{-3}$	12 mm
F9	7.069	0.23±0.039	0.1117±0.029	$11.7±0.023×10^{-3}$	17 mm

Journal of Chemical Health Risks
www.jchr.org
JCHR (2025) 15(6), 2618-2633 | ISSN:2251-6727

Table 10: Evaluation parameters of optimized batch F9 after stability study

Parameters	Initial (0 day)	After 60 days
Appearance	Transparent film	No changes
Weight (mg)	18 ± 3.6	19± 0.1
Thickness (mm)	0.23±0.03	0.23±0.09
Drug content (%)	95.91 ±0.01	95.99±0.05
Folding endurance	81.3±1.52	80±1.51
In-vitro disintegration (s)	21±4.11	21±3.98
Surface pH	6.7±0.06	6.8±0.04
Swelling index (%)	2.47± 0.12	2.12± 0.11
Water absorption ratio (%)	254.4±2.3	251.2±2.3

Conclusion:

A systematic DoE approach was used to develop an optimized fluconazole-loaded orodispersible film with ideal mechanical and disintegration properties. The optimized formulation, containing 2% polymer and 1.5% plasticizer, demonstrated rapid disintegration (21±4.11 s), high folding endurance (81.3±1.52), and efficient drug release with a T_{90}% of 18.81 minutes. The films also exhibited excellent drug entrapment efficiency (99.46±0.01%), enhanced permeability, and strong antifungal activity against *Candida albicans*. The formulation showed rapid disintegration, high drug entrapment, effective antifungal activity, and stability under accelerated conditions. Overall, these films (ODFs) offer a promising, patient-friendly alternative for treating oral fungal infections, with benefits like quick action and reduced side effects.

References:

1. Patel P, Limbashiya R, Chavd M, Shah U. Development and optimization of fast dissolving orodispersible film of Baclofen using 3^2 central composite design. International Journal of Pharmaceutical Sciences and Research. 2014; 5 (12): 5539-47. http://dx.doi.org/10.13040/IJPSR.0975-8232.5(12).5539-47
2. Aksungur P, Sungur A, Unal S, Iskit AB, Squier C A. Şenel S. Chitosan delivery systems for the treatment of oral mucositis: In-vitro and in-vivo studies. Journal of Controlled Release. 2004; 98(2): 269-279. https://doi.org/10.1016/j.jconrel.2004.05.002
3. Khlibsuwan R, Khunkitti W, Pongjanyakul T. Alginate-caseinate composites: Molecular interactions and characterization of cross-linked beads for the delivery of anticandidals. Int. J. Biol. Macromol. 2018; 115:483-493. https://doi.org/10.1016/j.ijbiomac.2018.04.095
4. Rongthong T, Sungthongjeen S, Siepmann J, Pongjanyakul T. Quaternary polymethacrylate–magnesium aluminum silicate films: molecular interactions, mechanical properties and tackiness. Int J Pharm. 2013 Dec 15;458(1):57-64. https://doi.org/10.1016/j.ijpharm.2013.10.016
5. Siriwachirachai C, Pongjanyakul T. Gelatinized tapioca starch−magnesium aluminum silicate nanocomposites: Physicochemical characterization and evaluation for modified-release tablets. J DRUG DELIV SCI TEC. 2023 Aug 1; 85:104591. https://doi.org/10.1016/j.jddst.2023.104591
6. Pereda M, Aranguren MI, Marcovich NE. Caseinate films modified with tung oil. Food hydrocolloids. 2010;24(8):800-808. https://doi.org/10.1016/j.foodhyd.2010.04.007
7. Pongjanyakul T, Priprem A, Puttipipatkhachorn S. Investigation of novel alginate−magnesium aluminum silicate microcomposite films for modified-release tablets. J. Contr. Release. 2005;107(2):343-356. https://doi.org/10.1016/j.jconrel.2005.07.003
8. Kajthunyakarn W, Khlibsuwan R, Sakloetsakun D, Pongjanyakul T. Sodium caseinate films modified using halloysite: Physicochemical characterization and drug permeability studies. J DRUG DELIV SCI TEC.2019; 54:101235. https://doi.org/10.1016/j.jddst.2019.101235
9. Glaessl B, Siepmann F, Tucker I, Siepmann J, Rades T. Characterisation of quaternary polymethacrylate films containing tartaric acid, metoprolol free base or metoprolol tartrate. Eur. J. Pharm. Biopharm.

Journal of Chemical Health Risks
www.jchr.org
JCHR (2025) 15(6), 2618-2633 | ISSN:2251-6727

2009;73(3):366-372. https://doi.org/10.1016/j.ejpb.2009.07.010
10. Wu C, McGinity JW. Non-traditional plasticization of polymeric films. Int. J. Pharm.1999;177(1):15-27. https://doi.org/10.1016/S0378-5173(98)00312-3
11. Varma N, Shaik SB. Formulation and evaluation of fast dissolving oral films of fluconazole by solvent casting technique. Indo Am. J. P. Sci.2021; 08(9): 216-223. https://doi.org/10.5281/zenodo.5515263
12. Pervaiz F, Mushtaq R, Noreen S. Formulation and optimization of terbinafine HCl loaded Chitosan/Xanthan gum nanoparticles containing gel: Ex-vivo permeation and in-vivo antifungal studies. J DRUG DELIV SCI TEC. 2021; 66:102935. https://doi.org/10.1016/j.jddst.2021.102935
13. Tundisi LL, Ataide JA, da Fonseca JHL, Silvério L AL, Lancellotti M, Paiva-Santos AC, Mazzola PG. Terbinafine nanohybrid: proposing a hydrogel carrying nanoparticles for topical release. Pharmaceutics. 2023;15(3): 841. https://doi.org/10.3390/pharmaceutics15030841
14. Rangel-Yagui CDO, Pessoa Jr A. Tavares LC. Micellar solubilization of drugs. J. Pharm. Pharm. Sci.2005;8(2):147-163.
15. Anusha RK, Sumana G. Formulation and evaluation of fast dissolving oral films containing baclofen. Asian J. Pharm. Educ. Res. 2023;12(3): 27-47. https://dx.doi.org/10.38164/AJPER/12.3.2023.27-47
16. Bajpai SK, Shah FF, Bajpai M, Jadaun M, Jyotish P. Dynamic release of amoxicillin from orally dissolving film (ODF) composed of casein and sodium alginate. J. Drug Res. Dev.2017;3(2): 1-7. https://doi.org/10.16966/2470-1009.134
17. Rençber S, Karavana SY, Yilmaz FF, Eraç B, Nenni M, Gurer-Orhan H, Ertan G. Formulation and evaluation of fluconazole loaded oral strips for local treatment of oral candidiasis. J DRUG DELIV SCI TEC.2019; 49:615-621. https://doi.org/10.1016/j.jddst.2018.12.035
18. Shinde SS, Shete AS, Patil MV, Varne BS. Different binary polymer mixture for solubility enhancement of poorly water-soluble drug by solid dispersion technique. International Journal of PharmTech Research.2012;4(3):1159-1166.
19. Hughey JR, Keen JM, McGinity JW. Investigating the formation of solid dispersions of poorly water-soluble drugs in hydrophilic carriers using thermal and spectroscopic techniques. *AAPS PharmSciTech.* 2010;*11*(3):1527–1534. https://doi.org/10.1208/s12249-010-9500-1
20. Syed SM, Marathe RP. Development and validation of UV spectrophotometric method for the estimation of fluconazole in the marketed dosage formulations. Pharm. Biosci. J. 2020;22-26. https://doi.org/10.20510/ukjpb/8/i5/1602587722
21. Niyaz Basha, Kalyani Prakasam, Divakar Goli. Formulation and evaluations of gel containing fluconazole-antifungal agent. Int. J. Drug Dev. & Res. 2011; 3(4): 109-128. https://www.ijddr.in/drug-development/formulation-and-evaluation-of-gel-containing-fluconazoleantifungal-agent.pdf
22. Alkhamis KA, Obaidat AA, Nuseirat AF. Solid-state characterization of fluconazole. Pharmaceutical development and technology. 2002;*7*(4):491-503. https://doi.org/10.1081/pdt-120015052
23. Zaki RM, Alfadhel M, Seshadri VD, Albagami F, Alrobaian M, Tawati SM, Almurshedi AS. Fabrication and characterization of orodispersible films loaded with solid dispersion to enhance Rosuvastatin calcium bioavailability. Saudi Pharmaceutical Journal. 2023;31(1): 135-146. https://doi.org/10.1016/j.jsps.2022.11.012
24. Yashaswini HN, Bhagawati ST, Manjunath K. Formulation and evaluation of fast dissolving buccal films containing bambuterol HCL. IJCSRR.2024;7(5): 2818-2833. https://doi.org/10.47191/ijcsrr/V7-i5-43
25. Ammanage A, Rodriques P, Kempwade A, Hiremath R. Formulation and evaluation of buccal films of piroxicam co-crystals. Future Journal of Pharmaceutical Sciences. 2020;6: 1-11. https://doi.org/10.1186/s43094-020-00033-1
26. Bala R, Pawar P, Khanna S, Arora S. Orally dissolving strips: A new approach to oral drug delivery system. Int. J. Pharm. Investig. 2013;3(2):67. https://doi.org/10.4103/2230-973X.114897

27. Reza HM, Islam T, Shohel M, Jain P. Formulation design and evaluation of baclofen mouth dissolving tablets. European Journal of applied sciences.2012;4(3):110-116. https://doi.org/10.5829/idosi.ejas.2012.4.3.669
28. Nadendla RR. Formulation and evaluation of glibenclamide oral fast dissolving films. Eur. J. Biomed.2016;3(5):535-542.
29. Khalbas AH, Albayati TM, Ali NS, Salih IK. Drug loading methods and kinetic release models using of mesoporous silica nanoparticles as a drug delivery system: A review. South African Journal of Chemical Engineering. 2024 Oct 1;50(1):261-80. https://doi.org/10.1016/j.sajce.2024.08.013
30. Berkow EL, Lockhart SR, Ostrosky-Zeichner L. Antifungal susceptibility testing: current approaches. Clin Microbiol Rev. 2020;33(3): 10-1128. https://doi.org/10.1128/CMR.00069-19
31. Udom IA, Owowo EE, Udofia LE. Antibiotic profile and molecular characterization of typhoidal salmonellosis among abattoir workers in the southern region of nigeria. Open Journal of Medical Microbiology.2023;13(1): 1-16. https://doi.org10.4236/ojmm.2023.131001
32. Sharma S, Naman S, Goyal K, Baldi A. Simultaneous estimation of atovaquone and mefloquine hydrochloride: QbD based method development and validation. Indian J. Pharm. Educ. Res.2023; 1;57(1):250-63. https://doi.org10.5530/001954641318
33. Shakya S. Formulation and optimization of immediate release tablet of sitagliptin phosphate using response surface methodology. Int J Pharm Biol Med Sci.2015; 4:7-12.
34. ICH I. (2023). Q2 (R2) Guideline on Validation of Analytical Procedures. ICH: Geneva, Switzerland. https://database.ich.org/sites/default/files/ICH_Q2(R2)_Guideline_2023_1130.pdf
35. Delgado R. Misuse of beer–lambert law and other calibration curves. Royal Society open science. 2022 Feb 2;9(2):211103. https://doi.org10.1098/rsos.211103
36. Kraisit P, Yonemochi E, Furuishi T, Mahadlek J, Limmatvapirat S. Chitosan film containing antifungal agent-loaded SLNs for the treatment of candidiasis using a Box-Behnken design. Carbohydrate Polymers. 2022; 283:119178. https://doi.org/10.1016/j.carbpol.2022.119178